Proceedings of the 2023 International Conference on Mechatronics and Smart Systems
DOI: 10.54254/2755-2721/12/20230255

Design and analysis of a new deployable platform based on scissor-like elements

Tianhong Bu [1, †], Hequn Kang [2, 4, †] and Jinyan Zhu [3, †]

[1] School of Engineering, RMIT University, Melbourne, VIC, 3000, Australia
[2] School of Mechanical Engineering, Jiangnan University, Wuxi, Jiangsu, 214000, China
[3] Shenzhen Middle School, Shenzhen, Guangdong, 518000, China

[4] 1043200127@stu.jiangnan.edu.cn
[†] These authors contributed equally.

Abstract. Conventional lifting platforms have a fixed operating table and due to space constraints, the operator needs to come back up and down to get the appropriate tools and materials. This paper proposes research into the development of lift platforms by using two different scissor-like elements to increase the utility rate of space and the stability of the whole system. Through parametric and kinematical analysis with a practical deployment simulation in modeling software. After analysis, research found that when the lifting platform rises at a constant speed, the speed of the protection net is first fast and then slow. When this mechanism rises, the height of the mechanism increases and the radius of the protection net changes in a circular curve, this study also found this platform is stable and easy to operate. This paper fully illustrates the great potential of this new lifting platform in the field of civil and aerospace engineering.

Keywords: deployable platform, scissor-like elements, lifting platform, double chain, sarrus linkage.

1. Introduction

The deployable structure is a new research frontier in traditional mechanics and is a new type of engineering structure with a wide range of applications in aerospace and civil engineering [1]. As shown in Figure. 1 (a), traditional expandable mechanisms are Scissor-like elements [2], double chain and 3D ring linkages. Among all these structures, the scissor-like elements are widely used in daily life as a lifting system due to their simple construction and low cost. By changing the scissor lever's angle, the structure's longitudinal length would increase, thus achieving a deployable effect. The closed loop double chain linkage is also used extensively in industry. The orderly discharge of the hinges results in a regular geometry. When not in use, it can be closed to form a smaller folding mechanism, and when in use, it can form a larger circle.

A large body of literature has extensively defined and designed lifting platforms. To increase the stability of the lifting platform, Cornel et al. added a hydraulic damping system to the bottom of the scissor structure to counteract the vibrations above the platform. At the same time, the hydraulics could

© 2024 The Authors. This is an open access article distributed under the terms of the Creative Commons Attribution License 4.0 (https://creativecommons.org/licenses/by/4.0/).

DOI: 10.54254/2755-2721/12/20230255

give additional support to the lifting platform to meet the greater force requirements [3]. However, hydraulic struts are expensive and have a higher failure rate than traditional mechanical structures. The operating platform of a conventional lift is a simple block of steel plate. Due to the limitations of the scissor-like element, the platform does not provide a larger area for storing tools and work materials, and the worker has to repeatedly ascend and descend to obtain the tools and materials required. There is no literature on the use of deployable structures to replace conventional steel plates.

At the same time, the single deployable structure has its limitations. These elements can only deform and stretch on two axes. When the structure is fully expanded, its transverse length becomes very short, resulting in reduced lateral stability, which can cause accidents in bumpy and rough conditions. A new combined 3D structure is required to develop. Machine enclosures or protective nets must frequently be open for routine maintenance and cleaning. In general, the shell or protective net of the machine is fixed with screws, which makes the system difficult to disassemble. To solve this complex and cumbersome disassembly, a deployable and liftable mechanism based on the scissor lift platform is designed. This mechanism allows the parts or items stored inside to be pushed out while the protective net is opened. It can solve the problem of the difficulty of removing parts from traditional lift platforms and will make up for the narrow range of applications of the common scissor-like lift platforms on the market.

The whole system will be assembled using different scissor-like elements, and the entire device can be divided into two parts. It will solve the problem of difficulties in dismantling parts of conventional lifting platforms and will make up for the lack of scope of application of the common scissor lift platforms on the market (as shown in Figure 1(b)) [4].

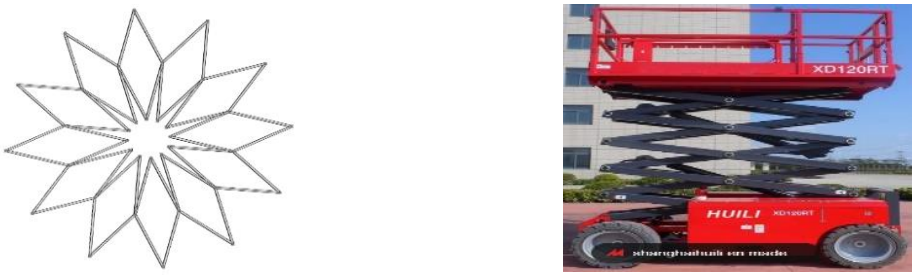

(a) (b)

Figure 1. Closed loop double chain linkage (a) and Scissor lift platform (b).

This paper is divided into four sections, including an introduction, construction of prototypes, model design with analysis methods and conclusion. Section 2 shows the whole prototypes of our design with all detailed constructions. The moving mechanism is introduced as well. Section 3 represents the quantitative calculations with all defined specific values. The conclusion part is presented in Section 4.

2. Construction of prototypes

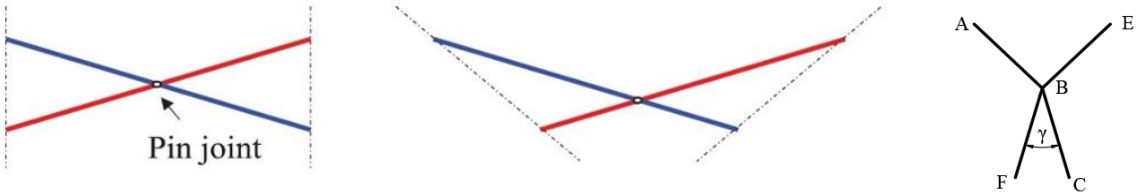

(a) (b) (c)

Figure 2. Types of scissor-like elements: translational (a), polar (b) [5], angulated scissor units (c).

Kim et al. summarized some common types of scissor-like elements [5]. The main types used in this study are the translational units and angulated scissor units shown in Figures 2 (a) and (c). These units are usually hinged by two rods, and these two rods can rotate relative around the hinge point.

DOI: 10.54254/2755-2721/12/20230255

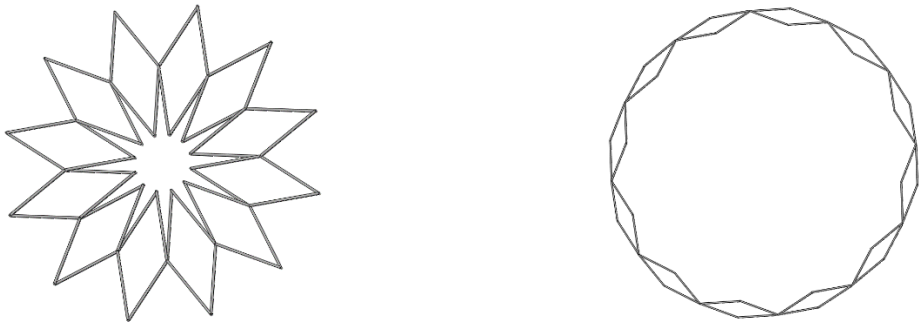

(a) (b)

Figure 3. The protective net when γ is equal to 10˚ (a) and 100˚ (b).

The protection net consists of multiple elements in Figure 2 (c), the points E and C of the first element are hinged to points A and F of the second element, respectively, and subsequent elements are connected in this way. Until points E and C of the last unit are hinged with points A and F of the first unit, respectively, the closed-loop double chain as shown in Figure 3 can be obtained. The joints such as A, B, C, E and F are all revolute joints. Using the *Kutzbach criterion*, the degree of freedom of the protection net is zero [9], but You, Z et al. have proved its mobility and only one degree of freedom [6]. When the included angle γ of the scissor-like element in Figure 2 (c) changes, the protective net expands or contracts, such as in Figures 3 (a) and (b).

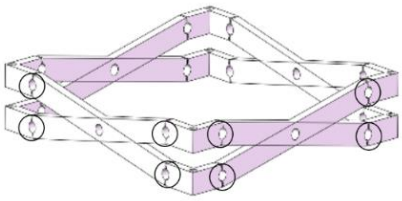

Figure 4. The unit of lifting device composed of scissor-like elements.

The four translational scissor-like elements in Figure 2 (a) constitute the basic unit of the lifting platform, and the joints marked in Figure 4 are revolute joints. Because this kind of lifting device can only lift in the vertical plane, it has only one degree of freedom.

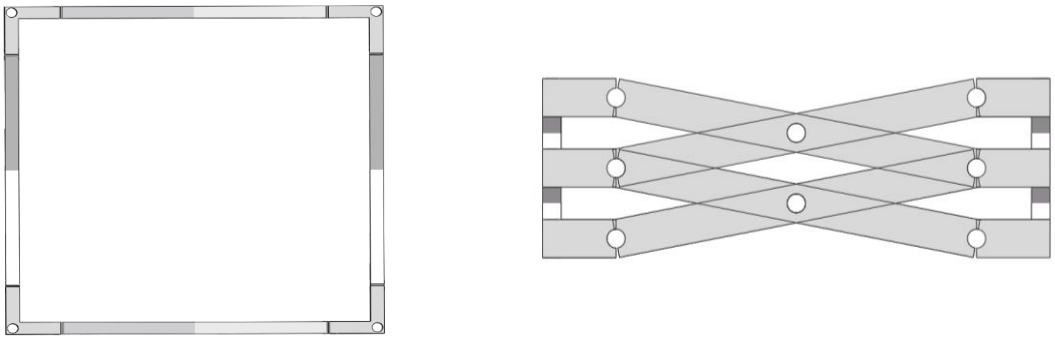

(a) (b)

Figure 5. Top views of the *Sarrus* linkage (a) and front views of the *Sarrus* linkage (b).

DOI: 10.54254/2755-2721/12/20230255

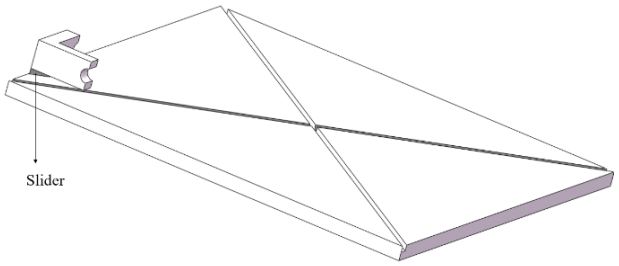

Figure 6. Schematic diagram of the position of the slider and the diagonal of the bottom quadrilateral.

In the top view, the area enclosed by the quadrilateral decreases as the platform height increases. As the lifting platform goes up, the bottom vertices move along the diagonal at the same time. Therefore, it is necessary to install a pulley at each of the four vertices at the bottom of the lifting device to ensure the normal operation of the lifting platform.

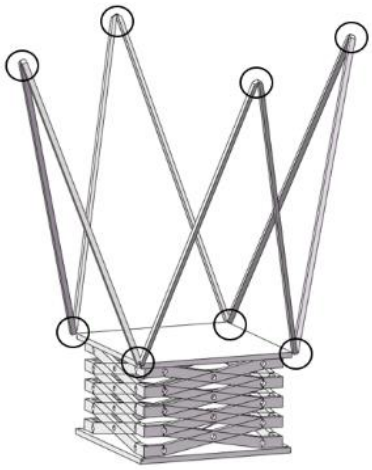

Figure 7. Schematic diagram of the support rod and related joints.

The protective net and the lifting device are connected through the support rod in Figure 7. These rods are connected to each other by ball joints and are connected with the protection net and the load platform respectively through the ball joints. Since overlapping of multiple ball joints in the same plane reduces the redundant degrees of freedom, the degree of freedom of the entire lifting platform with the protective net is one.

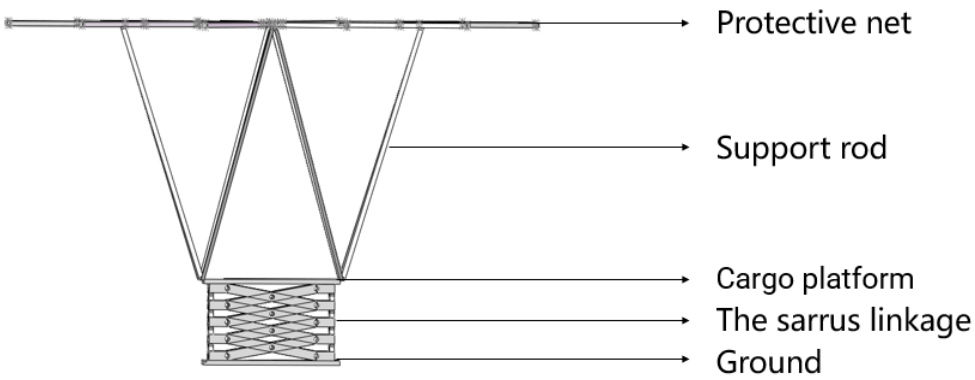

Figure 8. Model structure diagram.

As shown in Figure 8. The platform consists of two parts. The first part is the protective net. This part is deployable. The second part is a lifting platform, which can cause height changes by adjusting the angle of scissor-like elements. These two parts are connected by four links to increase stability. The height change of the lower *Sarrus* link drives the upper double chain to open and close through the link

DOI: 10.54254/2755-2721/12/20230255

[7]. It should be noted that the height of the protective net to the ground is constant, which ensures that the opening and closing of the upper protective net can change periodically with the height of the platform [8].

3. Model design and analysis methods

The analysis of the new deployable platform starts from two aspects. The first part is the parameter analysis of the initial state and the final state, and the second part is the kinematics analysis from the initial state to the final state [10].

3.1. Parametric analysis

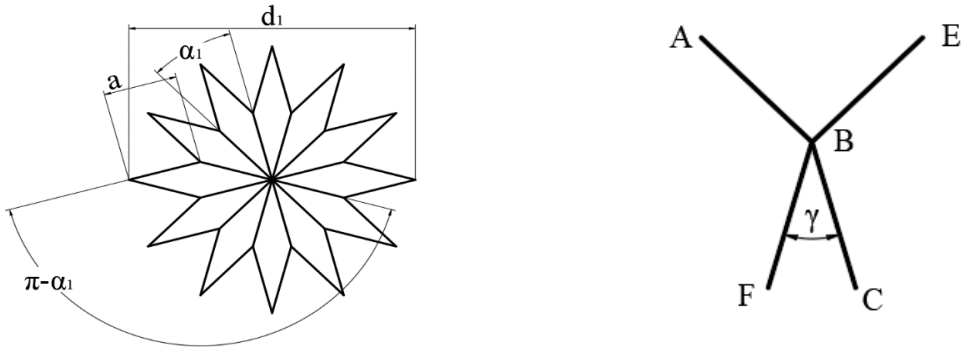

(a) (b)

Figure 9. Parameter diagram of the protective net in the closed state (a) and its basic unit (b).

Define the angle γ of the unit as shown in Figure 9 (b) in the initial state is equal to zero. The relationship between the number of units n_1 and the angle of α_1 can be solved as:

$$\alpha_1 = \frac{360^\circ}{n_1} \tag{1}$$

Calculate the maximum circumscribed circle diameter in the initial state shown in Figure 9. The expression for the diameter d_1 can be expressed by the length of the unit and the angle α_1.

$$d_1 = 2a\cos\frac{\alpha_1}{2} \tag{2}$$

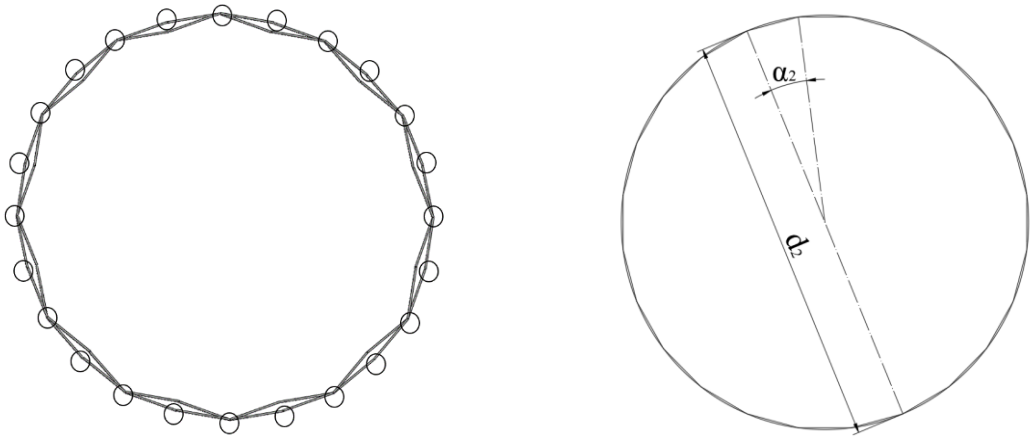

(a) (b)

Figure 10. The diagram of the protection net when deployed (a) and the marked points and related parameters (b).

For the parameter analysis in the end state, define that all the marked points of the protection net in the end state, as shown in Figure 10 (a), are located on the same circle. The loading platform and the

DOI: 10.54254/2755-2721/12/20230255

protection net are coincident at the same time. Then the angle α_2 marked in Figure 10 (a) can be calculated by Eqn.3.

$$\alpha_2 = \frac{2\pi}{2n_1} = \frac{\pi}{n_1} \tag{3}$$

As shown in Figure 10 (b), the diameter d_2 of the circumscribed circle can be expressed by a and α_2:

$$d_2 = \frac{a}{sin\left(\frac{\alpha_2}{2}\right)} \tag{4}$$

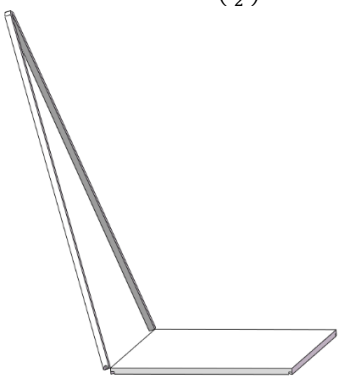

Figure 11. Schematic diagram of the support rod and platform shown in isolation.

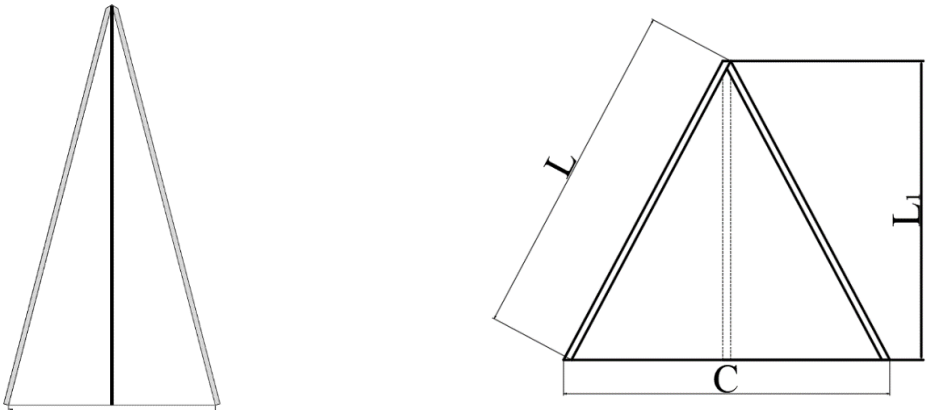

(a) (b)

Figure 12. Front view of the side of the support rod (a) and related parameters graph (b).

The function of two support rods with length L is theoretically equivalent to the support rod with length L_1 as shown in Figure 12, so for the convenience of calculation, they are equivalently replaced. This equivalent rod is perpendicular to the sideline of the loading platform, the vertical foot is the midpoint of the sideline of the loading platform, and the other end is connected with the protective net.

To ensure that the protection net can be unfolded and closed according to a predetermined period with the height change of the loading platform, it is defined that the diameter d_1 of the circumcircle of the protective net under complete closure is greater than the platform inscribed circle diameter C.

The relationship between the rod length L the equivalent rod length L_1 and the platform side length C can be expressed by Eqn.5.

$$L^2 = \left(\frac{C}{2}\right)^2 + {L_1}^2 \tag{5}$$

DOI: 10.54254/2755-2721/12/20230255

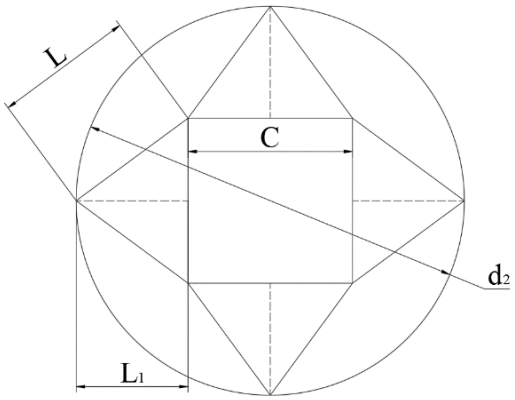

Figure 13. Top view of the parameters of the mechanism when the protective net is fully unfolded.

As Figure 13 shows, the relationship between the equivalent rod length *L*, the side length *C* of the cargo platform, and the diameter d_2 of the fully unfolded protective net's circumcircle can be shown by Eqn.6.

$$L_1 + \frac{C}{2} = \frac{d_2}{2} \tag{6}$$

The relationship between *L* and d_2, *C* can be obtained by combining Eqn.5 and Eqn.6 as:

$$L^2 = \left(\frac{C}{2}\right)^2 + \left(\frac{d_2}{2} - \frac{C}{2}\right)^2 \tag{7}$$

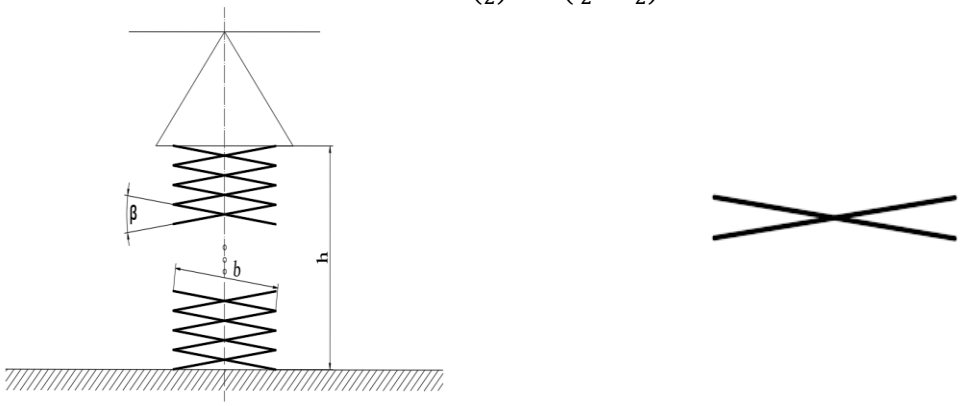

(a) (b)

Figure 14. Parameter diagram of the lifting device (a) and constituent units of *Sarrus* linkage (b).

For the lifting device, the relationship between the height *h* from the platform to the ground, the included angle of scissor-like element *β,* and the length *b* of scissor-like elements in the *Sarrus* linkage can be shown as Eqn.8.

$$h = n_2 \cdot b \cdot sin\frac{\beta}{2} \tag{8}$$

DOI: 10.54254/2755-2721/12/20230255

3.2. Kinematical analysis

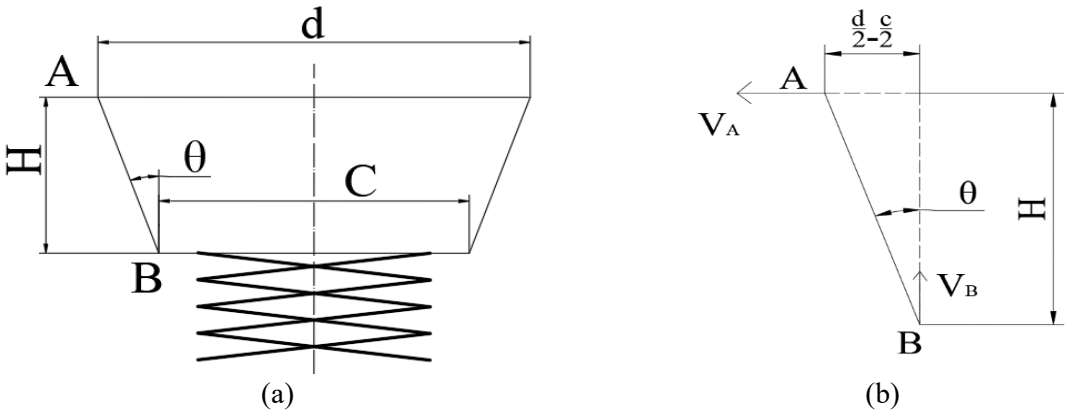

Figure 15. Parameter diagram of the front view of the mechanism (a) and the velocity vector analysis diagram of the equivalent rod (b).

$$cos\,\theta = \frac{H_0 - V_B t}{L_1} \tag{9}$$

The ratio of the speed of point A to the distance from A to the instantaneous center is equal to the ratio of the speed of point B to the distance from B to the instantaneous center as shown in Figure 15. Then the relationship between the velocity V_A at point A and the velocity V_B at point B can be expressed by θ, the diagram d of the protective net, and the length C of the platform as Eqn.10.

$$\frac{V_A}{(\frac{d}{2}-\frac{c}{2})tan\theta} = \frac{V_B}{\frac{d}{2}-\frac{c}{2}} \tag{10}$$

which can be simplified as Eqn.11.

$$V_A = \frac{V_B}{tan\theta} \tag{11}$$

The vertical distance H from the protective net to the loading platform is equal to the initial height H_0 minus the height of the loading platform rising, and the relationship can be shown by Eqn.12.

$$H = H_0 + tV_B \tag{12}$$

Then, according to the Figure 15 (a), the relationship of H_0 can be calculated by:

$$\left(\frac{d_1}{2} - \frac{c}{2}\right)^2 = {L_1}^2 + {H_0}^2 \tag{13}$$

Combining Eqn.9, Eqn.11, Eqn.12 and Eqn.13, the relationship between the expansion speed of the protection net V_A and time t can be obtained as Eqn.14.

$$V_A = \frac{V_B}{\sqrt{\frac{{L_1}^2}{(H_0 - V_B t)^2} - 1}} \tag{14}$$

The related kinematic images can be obtained in Figure 16. It can be seen that as the time increases, the speed of deployment of the protective net slows down and becomes zero when t equals 10 seconds, meaning that the net is fully deployed at this point.

DOI: 10.54254/2755-2721/12/20230255

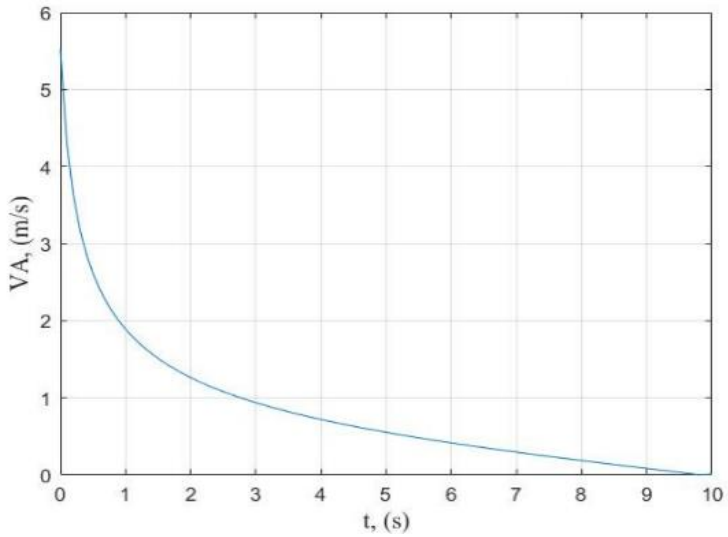

Figure 16. The relationship between the expansion speed of the protection network V_A and time t when n_1 is equal to 12, V_B is equal to 1 m/s, and L_1 is equal to 10 m.

As shown in Figure 15 (a), the size of the lifting distance H can be obtained as Eqn.15.

$$(H_0 - H)^2 + \left(\frac{d}{2} - \frac{c}{2}\right)^2 = {L_1}^2 \tag{15}$$

Then the relationship between the diameter d of the protection net and the height H of the loading platform can be obtained.

$$(10 - H)^2 + \left(\frac{d}{2} - 1\right)^2 = 100 \tag{16}$$

The related kinematic images can be obtained in Figure 17. The length of the loading platform increases with the increasing diameter of the protective net. By looking at Eqn.16, it is easy to see that the relationship between d and H appears as a quadratic arc.

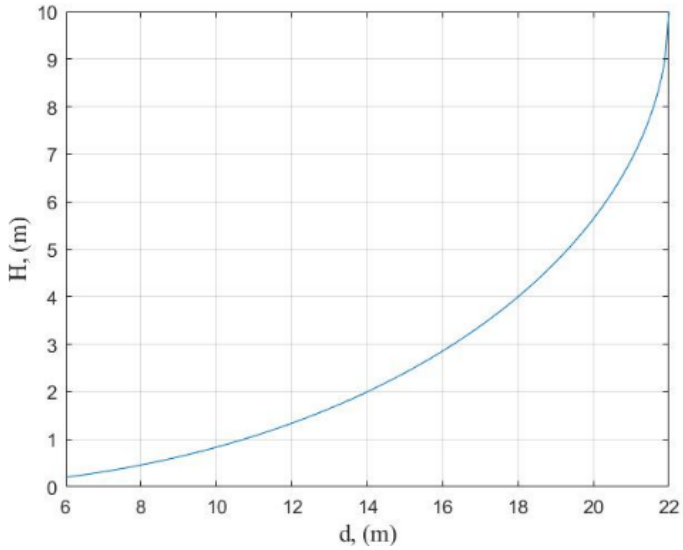

Figure 17. The relationship between the diameter d of the protection net and the height H of the loading platform when C is equal to 6m and L_1 is equal to 10m.

DOI: 10.54254/2755-2721/12/20230255

In addition, the relationship between the height h of the lifting platform and the unit angle β can be obtained in Figure 18. In line with the relationship between d and H, the height of the Sarrus linkage increases as the angle of scissor-like elements increases, and they both exhibit a sinusoidal relationship. As the angle of scissor-like elements cannot be greater than 90 degrees (1.5 radians), the height of the *Sarrus* linkage reaches the maximum value when the angle is 90 degrees.

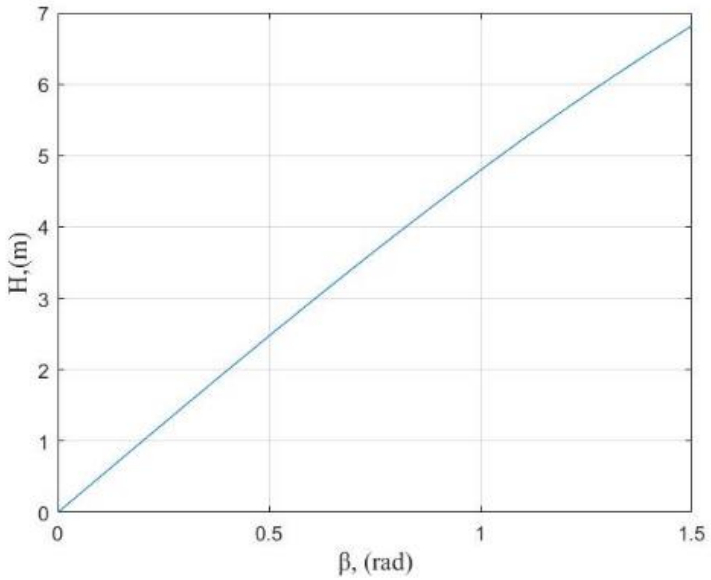

Figure 18. The relationship between the height h of the *Sarrus* linkage and the angle β of scissor-like elements when h_0 is equal to 5m, n_2 is equal to 5, and b is equal to 2m depends on Eqn.8.

4. Conclusion

This research proposes a combination of the *Sarrus* linkage and the closed loop double chain linkage. Then the research analyses the kinematic relationship between components of the structure by establishing mathematical models and acquiring a series of varying data with digital simulations. Analysis shows that when the lifting platform rises with constant speed, the speed of the protective net gradually decreases, this increases the efficiency of operation. When the mechanism rises, the height of the mechanism increases and the radius of the protective net varies following a circular curve. Under this circumstance, the platform is stable and easy to operate. Within the range of restrained parameters, the entire mechanical structure can be deployed and retracted. When retracted, the protective net provides protection for the internal device. And in the deployed state, the protective net is opened and the cargo platform is extended to the working position. After calculation, the maximum height of this lifting device can reach three to four times the initial height. While the maximum spread radius of the protection net is two to three times of the closed state. The specific telescopic multiplier of this lifting device can be adjusted by changing the length of the support rod L and the length of the protection net unit a to meet various scenarios. This mechanism can be applied in satellite antennas and payload protection, further usage of this mechanism is also to be discovered.

References

[1] Qi'an, P., Sanmin, W., Changjian, Z., & Bo, L. (2019). A New Flexible Multibody Dynamics Analysis Methodology of Deployable Structures with Scissor-Like Elements. Chinese journal of mechanical engineering., 32(5): 107-116.

[2] Luo, Y. Z., Mao, D.C., You, Z. (2007). On a type of radially retractable plate structures. International journal of solids and structures., 44(10): 3452-3467.

[3] Ciupan, C., Ciupan, E., Pop, E., Leordean, D., & Balc, N. (2019). Algorithm for designing a

DOI: 10.54254/2755-2721/12/20230255

hydraulic scissor lifting platform. In: MATEC Web of Conferences. pp. 299: 3012.
[4] Kumar, M. K., Chandrasheker, J., & Manda, M. (2016). Design & Analysis of Hydraulic Scissor Lift. International Research Journal of Engineering and Technology (IRJET)., 3(6): 1647-1653.
[5] Kim, Tae-Hyun; Suh, Jong-Eun; Han, Jae-Hung. Deployable truss structure with flat-form storability using scissor-like elements.[J].Mechanism & Machine Theory,2021,Vol.159: 104252
[6] Mao, D, C., Luo, Y. Z., & You, Z. (2009) Planar closed loop double chain linkages. Mechanism and Machine Theory., 44(4): 850-859.
[7] Li, Y. W., Wang, L. M., Liu, J. F., & Huang, Z. (2013). Applicability and Generality of the Modified Grübler-Kutzbach Criterion. Chinese journal of mechanical engineering., 26(2): 257-263.
[8] Liu, R., Yao, Y. A., & Li, Y. Z. (2020). Design and analysis of a deployable tetrahedron-based mobile robot constructed by Sarrus linkages. Mechanism and machine theory., 152: 103964.
[9] Mou, D. J., Zhang, Y. T., & Zhang, X (2018). Relationship and fundamental differences between degree of freedom of mechanism and components. Journal of Mechanical Engineering., 5: 74-83. (In chinese)
[10] Chai, T. J., Tan, C. S., Mohammad, S., Woon, K. S., Lim, M. H., Leong, K. H., Lau, S. H., Lee, M. L., Huang, Y. F., & Lee, Y. L. (2022). Structural performance of half scissor-like elements deployable structure. In: E3S web of conferences. pp. 1005.